Band gaps of GaPN and GaAsN alloys

L. Bellaiche, S.-H. Wei, and Alex Zunger

Band gaps of GaPN and GaAsN alloys

L. Bellaiche,[a] S.-H. Wei, and Alex Zunger
National Renewable Energy Laboratory, Golden, Colorado 80401

The importance of atomic relaxations, chemical disorder, and epitaxial constraints on the band gap of random, anion-mixed nitride alloys GaPN and GaAsN have been investigated, via pseudopotentials calculation. It has been demonstrated that simple approximations such as the virtual crystal approximation, or the use of high-symmetry ordered structure to mimic a random alloy, or the neglect of atomic displacements, are inadequate. It is found that a fully relaxed, large supercell calculation reproduces well the experimental band gaps of GaPN and GaAsN films. © *1997 American Institute of Physics.* [S0003-6951(97)01226-6]

Alloys of mixed-anion nitrides GaP–GaN and GaAs–GaN are different from most isovalent alloys, such as GaP–InP, GaAs–GaSb and GaAs–AlAs, in that the former systems exhibit in the dilute limit *deep band gap impurity levels*. Figure 1 shows the pseudopotential calculated,[1,2] energy levels of relaxed isolated substitutional anion impurities in GaN, GaP and GaAs. We see that when the atoms surrounding the impurity are allowed to relax, the P and As impurity atoms exhibit deep levels in the band gap of GaN, while N has no deep gap levels in GaP or GaAs.[1,2] Wei and Zunger,[3] and Bellaiche, Wei and Zunger[1,2] have shown that the existence of deep gap levels in the dilute alloy (''impurity'') limit alters the behavior of alloy states with composition, causing wave function localization on particular atoms in the cell,[1–3] anomalously large and composition-dependent optical bowing coefficients,[1,3] and a reduction of interband (dipole) transition probability.[2] These anomalous effects are fundamentally caused by the large chemical and size differences between N and the other column V anions it replaces. These large differences also invalidate some of the simple approximations used previously to describe the band gaps versus composition dependence in GaPN and GaAsN. For example, (i) the virtual crystal approximation (VCA) of Van Vechten *et al.*,[4] applied by Baillargeon *et al.*,[5] by Nakajima *et al.*,[6] and by Sakai *et al.*[7] to GaPN and GaAsN excludes at the outset the possibility of wave function localization on particular atoms by insisting that all anions in an alloy are identical (to a ''virtual'' anion), and by neglecting atomic relaxation. Similarly, (ii) approaches that model the random alloy via supercell structures neglecting the atomic relaxations (Ref. 8 for GaPN and Ref. 9 for GaAsN) can also misrepresent localization: Figure 1 shows indeed that in the absence of relaxation, N has spuriously deep gap levels in GaP and GaAs (dashed horizontal lines) that disappear, upon relaxation, into the host bands. Finally, (iii) using high-symmetry small-cell ordered structures to mimic the random alloys[10] could misrepresent atomic relaxation and electronic level repulsion.

We study here, using a large supercell (512 atoms) empirical pseudopotential approach (EPM), the different physical factors controlling the band gap versus composition behavior in GaPN and GaAsN alloys. We do this by starting with a general approach that includes most physical effects,

and then we ''tune out'' selectively some physical effects (atomic relaxation, chemical differences, symmetry), thus inferring their effects on the calculated properties.

Our most general, ''bottom line'' calculation will be described first. We model a random alloy by randomly occupying the anion sites of a large 512-atom ''supercell'' (containing 4×4×4 conventional cubic unit cells) by the alloyed atoms (e.g., P and N in GaP$_{1-x}$N$_x$). We then permit all atoms in the random configuration to relax to their minimum energy positions by minimizing the atomic strain energy. The lattice constant is assumed here to vary linearly as function of the composition x, as actually found for GaAs$_{1-x}$N$_x$ in relaxed local density approximation (LDA) total energy calculations.[3,10] The strain energy is modeled via the valence force field approach, fitted[1] to first-principles total energy calculations. Having obtained an equilibrium, relaxed random configuration of a large, periodic unit cell, we compute its band structure by the plane-wave pseudopotential method described in Ref. 1. We use local, screened pseudopotentials fit to band structures, deformation potentials and calculated band offsets. The resulting alloy band structure is then averaged over a few, random configurations.
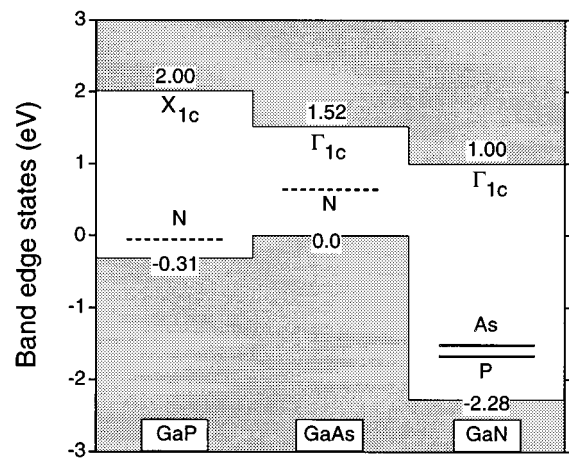
FIG. 1. Pseudopotential calculated deep gap levels at the dilute impurity limit in bulk GaP, GaAs, and GaN. The deep gap levels predicted in the presence (absence) of atomic relaxations around the impurity atom are indicated by thick solid (dashed) lines. The levels are fully occupied. The zero of energy is taken at the top of the valence band of pure GaAs. The natural band offsets are calculated by local density approximation (see Ref. 1).

---

[a]Electronic mail: laurent@sst.nrel.gov

FIG. 2. Calculated $T=0$ K bulk band gaps of (a) $GaP_{1-x}N_x$, and (b) $GaAs_{1-x}N_x$ alloys as a function of the nitrogen composition x. VD-Γ and VD-X denote the direct and indirect volume deformed energy gaps [Eq. (1)]. *VCA*, *unrelaxed* and *relaxed* refer to the VCA, the super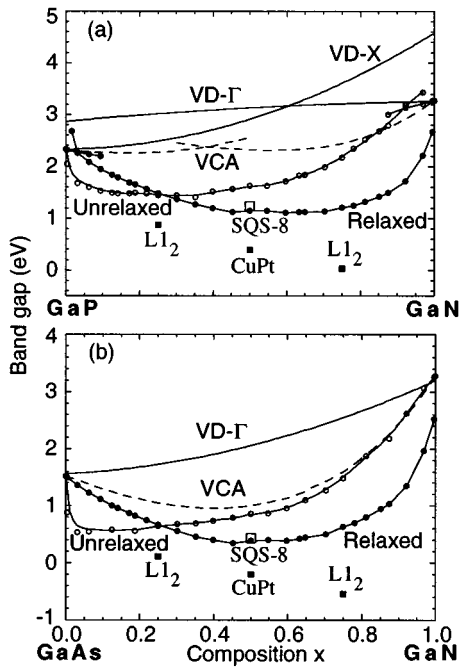cell calculations for unrelaxed random alloys, and the supercell calculations for relaxed random alloys, respectively. The symbols $L1_2$ and CuPt refer to various long ordered structures defined in Ref. 13. We also show the band gap for the 16 atoms "special quasirandom structure" [SQS-8 (Ref. 11)].

The whole calculation is then repeated for different alloy compositions. This gives us the band gap versus composition curves shown as solid lines connecting solid dots in Fig. 2. This type of calculation allows for the following physical effects: (1) wave function localization,[1,2] (2) atomic relaxation, (3) multiband coupling, and (4) the existence of a distribution of many local chemical environments (e.g., Ga coordinated by N_4, N_3P, N_2P_2, NP_3 and P_4) found previously to be crucial[11] for a correct description of the random alloys. This calculation neglects, however, short-range order in the form of atomic clustering. This effect will be discussed in a separate publication.[12]

To shed some light on the relative importance of physical factors affecting the composition dependence of the band gap, we now take a few steps backwards, and resolve our "bottom line result" into its simpler ingredients.

First, we imagine a crude model of the alloy in which only hydrostatic effects are taken into account: We model the "volume-deformed" (VD) band gap (of $GaP_{1-x}N_x$, for example) as

$$E_g^{VD}(x) = (1-x)E_g^{GaP}[V(x)] + xE_g^{GaN}[V(x)], \qquad (1)$$

where $V(x)$ is the volume of the alloy at composition x, taken from the Vegard's law. In this model, both chemical and relaxation effects are neglected, and the alloy is assumed to have the zincblende structure. Since GaP is compressed and GaN is dilated, their individual band gaps increase and decrease, respectively. The hydrostatic approximation of Eq. (1) gives the band gap denoted VD in Fig. 2. Notice small

bowing in the "volume deformed" band gap, and an indirect-to-direct crossover in $GaP_{1-x}N_x$ above $x_c=60\%$ nitrogen.

Second, we take GaP and GaN, already "prepared" in the previous step at the alloy volume $V(x)$, and mix them randomly in our 512-atom supercell, but preserve the ideal zincblende atomic positions, without relaxations. Thus, the Ga–N and Ga–P bond lengths are assumed in this step to be equal. This calculation already includes the *chemical effect* arising from the existence of a distribution of N and P atoms, but neglects *size differences*. The results of this calculation are denoted in Fig. 2 as "unrelaxed." Since, by Fig. 1, nitrogen has a deep level in the band gap of GaP if relaxation is ignored, we see in Figs. 1 and 2 that the unrelaxed band gap changes *discontinuously* from pure GaP $(x=0)$ to $x=0+\epsilon$. For the unrelaxed calculation, the indirect-to-direct crossover composition x_c is around 90% nitrogen.

Third, we permit the atoms in the supercell to relax. This model thus includes both chemical and relaxation effects. The resulting band gap is now denoted in Fig. 2 as "relaxed." We see that atomic relaxation changes dramatically the optical bowing. Furthermore, the deep levels of nitrogen in GaP and GaAs (Fig. 1) disappear upon relaxation, and deep levels of P and As impurities appear in the gap of GaN (Fig. 1). Thus, the relaxed band gap shows now a discontinuous jump from $x=1$ (pure GaN) to $x=1-\epsilon$, but a continuous behavior from $x=0$ (pure GaP) to $x=0+\epsilon$. There is now a crossover between two conduction states of $GaP_{1-x}N_x$ at above 3% of nitrogen: below this composition the conduction band minimum (CBM) has a high X_{1c} character, while above this composition the CBM has a majority Γ_{1c} component.

Our calculation thus shows that both *chemical effects* (the difference between "VD" and "unrelaxed") and *size effects* (the difference between "unrelaxed" and "relaxed") affect profoundly the band gaps of GaPN and GaAsN alloys. Three additional conclusions emerge regarding the comparison with previous calculation methods:

(i) Using the same pseudopotential, we have calculated the band gaps of relaxed, *small unit cell ordered structures*: Ga_4P_3N ($L1_2$ structure), Ga_2PN (CuPt structure), and Ga_4PN_3 ($L1_2$ structure). The results are shown as solid squares in Fig. 2. We see that such long-range-ordered structures have a significant band gap reduction relative to the random alloy of the same composition (0.6 eV in Ga_2AsN and 0.75 eV in Ga_2PN in the CuPt structures). In fact, one can obtain a *negative* band gap in GaAsN if one assumes CuPt ordering.

(ii) Using our pseudopotentials we have also calculated the band gap predicted by the virtual crystal approximation (VCA). This approximation includes hydrostatic effects, partial chemical effects, but neglects structural relaxation. The results, shown as dashed lines in Fig. 2, are seen to be a very poor approximation to the large supercell, fully relaxed calculation, as also emphasized in Ref. 10: for example the direct/indirect crossover predicted by the VCA in GaPN occurs for a nitrogen composition close to 40%, which differs strongly from the 3% result obtained in the relaxed, large supercell calculation. Thus, we conclude that the VCA[5–7]
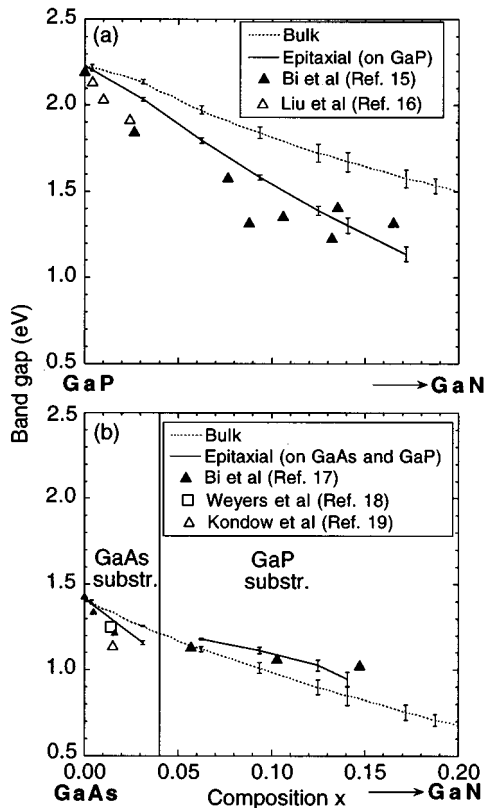
FIG. 3. Calculated $T=300$ K fully relaxed band gap of (a) GaPN, and (b) GaAsN alloys as a function of the nitrogen composition. The dashed line refers to bulk conditions, while the solid line correspond to epitaxial conditions (GaP substrate for GaPN alloys, and GaAs and GaP substrates for GaAsN alloys). The calculations are compared to different experimental results (see Refs. 15–19).

and the unrelaxed supercell calculations[8,9] are inappropriate for GaPN and GaAsN.

(iii) We next tested the ''special quasirandom structures'' (SQS) idea.[14] In this approach a small supercell with low site symmetry is designed to statistically mimic the atomic correlations in far larger *random* structures. Using the SQS-8 (SQS-16) structure (Ref. 11) we find band gaps of 1.23 (1.09) eV in $GaP_{0.5}N_{0.5}$ and of 0.44 (0.37) eV in $GaAs_{0.5}N_{0.5}$, which compared favorably with the 512 atom supercells calculation of 1.14 ± 0.07 eV and 0.39 ± 0.08 eV. Thus, the SQS construct is highly effective in that small, but specially selected unit cells reproduce remarkably well large unit cells.

Having understood the importance of relaxation, chemical effects and disorder on the band gap, we next compare our results with experiment. Since current experiments[16–20] are done on epitaxial films rather than on bulk alloys, we repeat our bulk calculation (Fig. 2) for epitaxial geometry. This is done by restricting the in-plane lattice constant to match that of the prescribed substrate (GaP for GaPN alloys, and both GaAs and GaP substrates for GaAsN alloys), and relaxing the supercell lattice constant in the tetragonal direction so as to minimize the energy. We thus assume *coherent* films, while in reality some of the coherence could be lost, depending on the thickness and on the composition of the films. We further correct our calculated $T=0$ K alloy results of Fig. 2 to room temperature used in Refs. 15 and 17. We

do so by using a composition-weighted band gap temperature shift of the constituents: 0.10 eV for GaP and GaAs, and 0.18 eV for GaN (measured[20,21] from low temperature to 300 K). We have also shifted the experimental results of Refs. 16, 18, and 19 to correct for the temperature dependence of the band gap from 5 K[16] or 77 K[18,19] to room temperature. Figure 3 shows our calculated, fully relaxed and temperature-corrected band gaps of $GaP_{1-x}N_x$ and $GaAs_{1-x}N_x$ in both epitaxial and in bulk geometries, compared with the measured results.[15–19] We see that the epitaxial conditions can change considerably the band gap of these alloys with respect to the bulk conditions. We also notice quite good agreement between our epitaxial calculations and experimental results, especially for larger N compositions.

In summary, we have pointed out that simple approximations such as the VCA, the use of high-symmetry small ordered structures to mimic random alloys, or the neglect of relaxation are inappropriate for describing the band gaps versus composition dependence in GaPN and GaAsN random alloys. This is due to the fact that these kinds of calculations misrepresent the band-edge wave function localization occurring in these alloys.[1–3] In addition, we found that our fully relaxed, large supercell calculations of epitaxial GaPN and GaAsN alloys differ considerably from the corresponding bulk results, and reproduce quite well the measured band gaps.

[1] L. Bellaiche, S.-H. Wei, and A. Zunger, Phys. Rev. B **54**, 17568 (1996).
[2] L. Bellaiche, S.-H. Wei, and A. Zunger, Phys. Rev. B (submitted).
[3] S.-H. Wei and A. Zunger, Phys. Rev. Lett. **76**, 664 (1996).
[4] J. A. Van Vechten, Phys. Rev. **182**, 891 (1969).
[5] J. N. Baillargeon, K. Y. Cheng, G. E. Hofler, P. J. Pearah, and K. C. Hsieh, Appl. Phys. Lett. **60**, 2540 (1992).
[6] S. Nakajima, H. Ohshiba, T. Yang, and S. Sakai, Jpn. J. Appl. Phys. 1 **35**, 5602 (1996).
[7] S. Sakai, Y. Ueta, and Y. Terauchi, Jpn. J. Appl. Phys. 1 **32**, 4413 (1993).
[8] S. Miyoshi and K. Onabe, Topical Workshop on Nitrides, 1996.
[9] A. Rubio and M. L. Cohen, Phys. Rev. B **51**, 4343 (1995).
[10] J. Neugebauer and C. G. Van de Walle, Phys. Rev. B **51**, 10568 (1995).
[11] S.-H. Wei, L. G. Ferreira, J. E. Bernard, and A. Zunger, Phys. Rev. B **42**, 9622 (1990).
[12] L. Bellaiche, S.-H. Wei, and A. Zunger (unpublished).
[13] Z. W. Lu, S. H. Wei, A. Zunger, S. Frota-Pessoa, and L. G. Ferreira, Phys. Rev. B **44**, 512 (1991).
[14] A. Zunger, S.-H. Wei, L. G. Ferreira, and J. E. Bernard, Phys. Rev. Lett. **65**, 353 (1990).
[15] W. G. Bi and C. W. Tu, Appl. Phys. Lett. **69**, 3710 (1996).
[16] X. Liu, S. G. Bishop, J. N. Baillargeon, and K. Y. Cheng, Appl. Phys. Lett. **63**, 208 (1993).
[17] W. G. Bi and C. W. Tu, Appl. Phys. Lett. **70**, 1068 (1997).
[18] M. Weyers, M. Sato, and H. Ando, Jpn. J. Appl. Phys. 1 **31**, L853 (1992).
[19] M. Kondow, K. Uomi, K. Hosomi, and T. Mozume, Jpn. J. Appl. Phys. 1 **33**, L1056 (1994).
[20] *Semiconductors–Basic Data*, 2nd revised ed., edited by O. Madelung (Springer, Berlin, 1996).
[21] S. Strite and H. Morkoc, J. Vac. Sci. Technol. B **10**, 1237 (1992).